### Analytical instrument engineering and technology Аналитическое приборостроение и технологии

UDC 621.383.2.032.12+681.586.7 https://doi.org/10.32362/2500-316X-2023-11-5-81-93



#### **RESEARCH ARTICLE**

### DC/DC converter to power spectral lamps

Mikhail Yu. Nikolshin <sup>1</sup>, Alexander V. Frunze <sup>2</sup>, Vladimir K. Bityukov <sup>1, ®</sup>

- <sup>1</sup> MIREA Russian Technological University, Moscow, 119454 Russia
- <sup>2</sup> TERMOKONT, Moscow, 119361 Russia

#### **Abstract**

**Objectives.** The paper describes the creation of a DC/DC converter for powering hollow cathode lamps widely used currently as highly stable sources of spectral lines in spectral absorption analyzers and other applications. Typically, mains power supplies are used for such lamps, since installations using hollow cathode lamps are manufactured as stationary. However, there are no principal obstacles to manufacturing portable versions by simply substituting the power supply. However, special attention should in this case be paid to the power supply of the spectral lamp itself, since the amplitude stability of the radiation depends on the smoothness of its supply voltage. Therefore, the development of the pulse DC/DC converter with high efficiency and low rippling is a relevant and expedient problem. **Methods.** The set task is solved by methods of mathematical calculations, circuit simulation in *LTSpice XVII* computer-aided design system, and experimental verification.

**Results.** The structural and principal electrical circuit of a prototype converter is developed on the basis of a topological analysis of pulse DC/DC converters, along with its calculations and simulation, and a printed circuit board. The developed autonomous high-voltage DC/DC converter has a low ripple level (~250 mV) of the output voltage (~491 V) at a load current of ~20 mA to ensure highly stable radiation.

**Conclusions.** The possibility of obtaining a high voltage when using the topology of a step-up DC/DC converter with a choke is demonstrated. The experimental verification confirmed the correctness of calculations and modeling of a high-voltage DC/DC converter for powering hollow cathode spectral lamps.

**Keywords:** hollow cathode spectral lamp, gas discharge lamp, pulse converter, DC/DC converter, high-voltage converter, simulation

• Submitted: 27.01.2023 • Revised: 07.05.2023 • Accepted: 13.07.2023

**For citation:** Nikolshin M.Yu., Frunze A.V., Bityukov V.K. DC/DC converter to power spectral lamps. *Russ. Technol. J.* 2023;11(5):81–93. https://doi.org/10.32362/2500-316X-2023-11-5-81-93

Financial disclosure: The authors have no a financial or property interest in any material or method mentioned.

The authors declare no conflicts of interest.

<sup>&</sup>lt;sup>®</sup> Corresponding author, e-mail: bitukov@mirea.ru

#### НАУЧНАЯ СТАТЬЯ

### DC/DC-преобразователь для питания спектральных ламп

М.Ю. Никольшин <sup>1</sup>, А.В. Фрунзе <sup>2</sup>, В.К. Битюков <sup>1, @</sup>

#### Резюме

**Цели.** Цель работы – создание DC/DC-преобразователя для питания ламп с полым катодом, которые в настоящее время широко используются в качестве высокостабильных источников спектральных линий в установках спектрального абсорбционного анализа и в иных случаях. Зачастую для таких ламп используются сетевые источники питания, т.к. установки с использованием ламп с полым катодом выполняются в стационарном исполнении. Однако препятствий принципиального характера для выполнения такого рода установок в переносном варианте нет. Для этого, в первую очередь, следует отказаться от привязки питания к сети переменного тока. Особое внимание при этом должно быть обращено на питание самой спектральной лампы, т.к. от пульсаций ее питающего напряжения зависит амплитудная стабильность излучения. Следовательно, разработка импульсного DC/DC-преобразователя с высоким КПД и малыми пульсациями является актуальной и целесообразной проблемой.

**Методы.** Поставленная задача решена методами математических расчетов, схемотехнического моделирования в системе автоматизированного проектирования *LTSpice XVII* и экспериментальной проверки.

**Результаты.** Выполнен анализ топологий импульсных DC/DC-преобразователей, разработаны структурная и принципиальная электрические схемы преобразователя, проведены их расчеты и моделирование, разработана печатная плата. Для обеспечения высокостабильного излучения разработан и создан автономный высоковольтный DC/DC-преобразователь, имеющий малый уровень пульсаций (~250 мВ) выходного напряжения (~491 В) при токе нагрузке ~20 мА.

**Выводы.** Показана принципиальная возможность получения высокого напряжения при использовании топологии повышающего DC/DC-преобразователя с дросселем. Экспериментальная проверка подтвердила корректность расчетов и моделирования высоковольтного DC/DC-преобразователя для питания спектральных ламп с полым катодом.

**Ключевые слова:** спектральная лампа с полым катодом, газоразрядная лампа, импульсный преобразователь, DC/DC-преобразователь, высоковольтный преобразователь, моделирование

• Поступила: 27.01.2023 • Доработана: 07.05.2023 • Принята к опубликованию: 13.07.2023

**Для цитирования:** Никольшин М.Ю., Фрунзе А.В., Битюков В.К. DC/DC-преобразователь для питания спектральных ламп. *Russ. Technol. J.* 2023;11(5):81–93. https://doi.org/10.32362/2500-316X-2023-11-5-81-93

**Прозрачность финансовой деятельности:** Авторы не имеют финансовой заинтересованности в представленных материалах или методах.

Авторы заявляют об отсутствии конфликта интересов.

<sup>1</sup> МИРЭА – Российский технологический университет, Москва, 119454 Россия

<sup>&</sup>lt;sup>2</sup> АНО НТП «Термоконт», Москва, 119361 Россия

<sup>&</sup>lt;sup>®</sup> Автор для переписки, e-mail: bitukov@mirea.ru

#### INTRODUCTION

Hollow cathode lamps are used to obtain highly stable spectra of certain wavelengths [1–5]. When a discharge occurs in a lamp of this type, its cathode and inert filler gas start emitting energy in the ultraviolet and visible spectral ranges. The wavelengths of radiation are determined by the composition of the filler gas and cathode alloy. For example, LF-6M lamp with zinc-coated cathode has the main spectral line of 229.6 nm.

Since a hollow cathode lamp is a gas discharge lamp according to its principle of operation, it follows that the essential nature of its discharge occurrence does not differ from that of other gas discharge lamps, such as indicator lamps with neon filling and gas-filled relays. However, indicators can tolerant a significant level of pulsations in their power supply, which is unacceptable for spectral lamps, since the pulsations of current flowing through the lamp cause changes in the amplitude of spectral components. Considering that spectral lamps are used in instrumentation, the intensity of the formed spectral components must be as stable as possible. Thus, the stability of the radiation intensity depends on both the properties of the lamp itself and the parameters of the supply voltage. However, a detailed consideration of the properties of the lamp affecting the stability of the radiation intensity, such as emission, purity of glass, durability, etc., are beyond the scope of the present paper.

The stability of power supply parameters can be achieved by using a negative feedback system [6]. For devices with spectral lamps, this may be achieved by introducing a negative feedback loop either for the lamp current consumption or for the level of the emitted luminous flux. Here, the reduction of the lamp emission ripple is largely related to the reduction of ripples in its supply voltage.

As a rule, devices using spectral discharge lamps are mains powered, which determines the stationary nature of their use. Such a power supply is traditionally carried out using a continuous regulation scheme according to which devices permit a relatively stable voltage having small ripples at the output. Moreover, issues of their efficiency and mass-dimensional parameters are not relevant. One of the implementations of such power supply for spectral lamps wherein the mains voltage multiplication principle is used for obtaining high voltage is proposed in [7].

However, the portable form-factor of using devices with a spectral lamp is also relevant and fundamentally possible. For such autonomous devices, it is advisable to use a switching power supply due to its smaller mass-size parameters in comparison with linear sources of secondary power supply.

# CONVERTER PARAMETERS AND ITS BLOCK DIAGRAM

Specifications for output voltage and load current of the DC/DC converter are determined by the parameters of manufactured Russian hollow cathode lamps shown in Table 1.

**Table 1.** Parameters of ignition voltage and amperage of Russian hollow cathode lamps

Lamp type	Ignition voltage, V	Lamp amperage, mA
LT-2	450	20
LV-2	300	20
LT-6M	500	12

The following basic requirements to the pulse converter for hollow cathode lamps may be formulated: output voltage  $\sim$ 500 V; load current  $\geq$ 0.02 A; output voltage ripple at current load 20 mA  $\leq$ 0.5 V; and input voltage  $\sim$ 15 V.

These parameters may be obtained using the DC/DC converter based on the classical step-up converter scheme (Fig. 1) [8, 9].

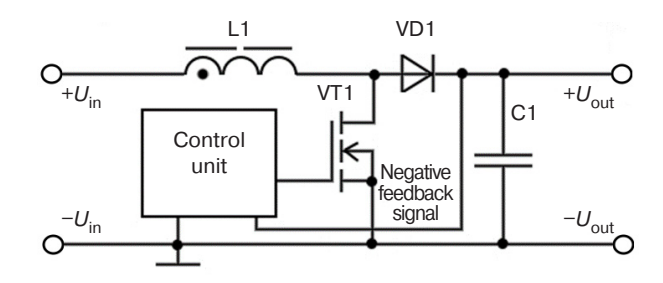


**Fig. 1.** The power section schematic diagram of the step-up DC/DC converter. Here and in the following figures, the designations of scheme elements correspond to the designations adopted in GOST 2.710-81<sup>1</sup>

The output voltage of the converter is regulated by pulse-width modulation (PWM) or pulse-frequency modulation (PFM). The features of these modulations are considered in [8–12].

The control unit changes the pulse duty factor—or ripple frequency—when the specified output voltage threshold is reached. The main element of the control unit circuit is the one that changes the duty factor upon reaching a certain output voltage threshold. The widespread integrated timer KR1441VI1<sup>2</sup> (TLC55 chip analog<sup>3</sup> being the NE555 CMOS version<sup>4</sup>), which

<sup>&</sup>lt;sup>1</sup> GOST 2.710-81. Unified system for design documentation. Alpha-numerical designations in electrical diagrams. Moscow: Izd. Standartov; 1985 (in Russ.).

<sup>&</sup>lt;sup>2</sup> Manufactured by Mikron, Zelenograd, Russia.

<sup>&</sup>lt;sup>3</sup> TLC555 datasheet. https://datasheet.lcsc.com/lcsc/2008261939\_ HGSEMI-TLC555N\_C725329.pdf. Accessed 20.05.2023.

<sup>&</sup>lt;sup>4</sup> A complementary metal-oxide semiconductor (CMOS) is the integrated circuit technology and circuit design based on *p*- and *n*-channel transistors with insulated gate.

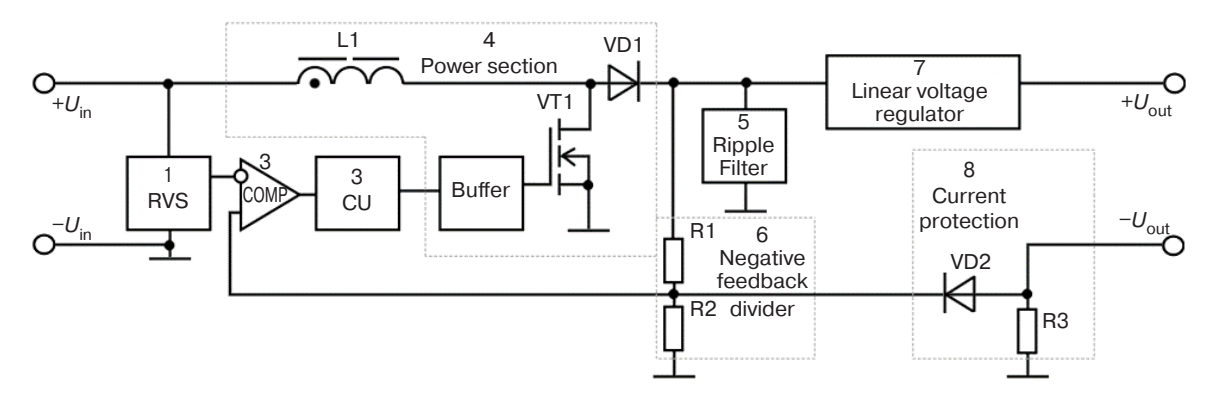


Fig. 2. Structural diagram of the DC/DC converter

can be switched into stable multivibrator mode, i.e., a rectangular pulse generator having a given duty cycle, may be used for this purpose. The adjustment of output voltage in the circuit is provided by changing current between the control pin (pin 5 for 8-pin case) and the circuit common wire. This would change the frequency of the output ripples. The bipolar transistor is used as the regulating element that changes the control pin current.

The circuit clearly recording the fact of reaching the specified voltage is required as the sensor that would detect the voltage of 500 V at the converter output. This is due to the fact that the control pin switch has an active mode area when it is not fully open, as well as a technological opening voltage spread. For example, one bipolar transistor may be fully open at 0.76 V, another at 0.78 V, the third at 0.75 V, etc. The voltage spread would cause the stabilization voltage spread, i.e., the transistor opening should be provided by a third-party circuit having the lowest actuation voltage spread.

A comparator, for example, K554SA301A<sup>5</sup> (LM311 analog<sup>6</sup>), may be used as such sensor to whose inverting input the reference voltage source (RVS) implemented on a parametric voltage regulator is connected, while to the non-inverting input the midpoint of the output voltage divider is connected, designed so that the voltage equal to the RVS output voltage would be at its midpoint at the input voltage of 500 V. When the voltage at the non-inverting input is exceeded, the comparator closes the built-in output transistor to set a high voltage level at the output. This high voltage opens the transistor connected to the control pin of the KR1441VI1 chip thus stopping the generation. When the output voltage drops below 500 V, the comparator changes its state due to the reference voltage level exceeding the divider output voltage, while the transistor closes causing the generation of ripples again.

The structural diagram of the converter is shown in Fig. 2.

The functionality of the DC/DC converter blocks marked by numbers in Fig. 2 is as follows:

- **1. RVS.** This is designed to form stable voltage being the reference voltage for actuating comparator 2 upon reaching the set output voltage.
- **2.** Comparator (COMP). As long as the voltage at the output of the negative feedback divider 6 is less than the voltage generated by RVS, the comparator has low voltage level at its output. The low voltage level at the control unit 3 input is responsible for ripple generation. When the voltage at the negative feedback divider 6 output exceeds the RVS level, the comparator sets high voltage level at the output which prohibits the control unit 3 from generating ripples.
- **3. Control unit (CU).** This generates rectangular pulses that control the power section 4 of the converter by switching MOSFET VT1<sup>7</sup> on or off.
- **4. Power section.** This consists of the choke L1 on which the induction EMF is induced, MOSFET VT1 commutating the right output of the choke L1 either to diode VD1 or to "ground", the rectifier diode VD1, and the buffer stage. The buffer stage is required for matching the low-current output stage of the control unit 3 with the high gate charge current of MOSFET VT1 when it opens and closes in a short time interval
- **5. Ripple filter.** This is designed for smoothing the output voltage.
- 6. Negative feedback divider. The divider division ratio determines the output voltage: when the voltage at the output of the negative feedback divider connected to the non-inverting input of comparator 2 becomes higher than the output voltage of RVS 1 (connected to its inverting input), comparator 2 would set high level while control unit 3 would stop generating ripples, thus stopping conversion until the comparator output level becomes low again. This is achieved only if the voltage at the output of divider 6 supported by capacitive filter 5 does not become lower than the voltage of RVS 1 again.

<sup>&</sup>lt;sup>5</sup> Manufactured by Mikron, Zelenograd, Russia.

<sup>&</sup>lt;sup>6</sup> LM311 datasheet. https://www.onsemi.com/pdf/datasheet/lm211-d.pdf. Accessed May 20, 2023.

<sup>&</sup>lt;sup>7</sup> The metal-oxide-semiconductor field-effect transistor (MOSFET) is a field-effect transistor with insulated gate.

The divider output voltage  $U_{\rm div}$  is determined by the following formula:

$$U_{\text{div}} = U_{\text{in}} \frac{R_2}{R_1 + R_2},\tag{1}$$

where  $U_{\rm in}$  is the input voltage of the divider (it is the converter output voltage in this circuit), while  $R_1$  and  $R_2$  are resistances of the negative feedback divider arms.

- 7. Linear stabilizer. For reducing the output voltage ripple level, a compensating voltage regulator with continuous regulation is used. Its scheme is shown in Fig. 3 (elements R16, VD6–VD10, VT7, and C7). The stabilizer output voltage is equal to the sum of stabilization voltages of stabilitrons VD6–VD10 plus the base-emitter voltage of transistor VT7 (about 0.5–0.7 V). Calculations have shown that, at a pulse converter output voltage of 530 V, a linear stabilizer output voltage of 500 V, and a load current 20 mA, power of 0.6 W would be dissipated on the control transistor.
- **8. Protection.** When the current exceeds the nominal value determined by the resistance of resistor R3, the voltage at the non-inverting input of comparator 2 becomes higher than the voltage level of RVS 1, which would cause the control unit 3 to stop generating ripples. This is essentially a parallel feedback channel. The diode VD2 is designed to prevent the current flow from the negative feedback divider 6 through resistor R3. The resistor R3 resistance is calculated based on the switching voltage of the comparator  $U_{\rm RVS}$ , the load current flow at which protection  $I_{\rm protect}$  actuates, and the direct voltage drop  $U_{\rm VD2~dir}$  across diode VD2 by the following formula:

$$R_3 = \frac{U_{\text{RVS}} + U_{\text{VD2 dir}}}{I_{\text{protect}}}.$$
 (2)

For the protection actuation current of 25 mA, the reference voltage of 3.3 V and the direct voltage drop across the diode of 0.6 V, the resistor R3 resistance is 156  $\Omega$ . This resistor is included in series with the load, and it would inevitably drop some of the output voltage. Operating voltage of spectral lamps ranges within 250-300 V, while the recommended current for maintaining the discharge is up to 2/3 of the maximum, i.e., 8–12 mA. It should be noted that the service life of spectral lamps is normalized in milliampere-hours, i.e., reducing the current increases not only the empirical, but also the documented service life of the lamp. The equivalent resistance of the lamp, accordingly, would be in the range from 20.8 to 37.5 k $\Omega$ . In the worst case, i.e., when the tube resistance is minimal, the voltage drop across R2 is calculated by formula (1) is 3.7 V, i.e., less than 1% of output voltage, which is totally unnoticeable in practice. If, however, the output voltage should precisely match the data sheet, it can be adjusted by setting the output voltage not at idle but under load,

which may be a resistor of equivalent resistance to that of a particular type of lamp.

It is worth detailing the selection of the type and rating of choke L1. The step-up converter has both continuouscurrent and discontinuous-current operating modes. The discontinuous-current mode means that the current flows through the choke L1 winding to all converter operation phases, which varies but never goes to zero. In discontinuous-current mode, the current through the choke L1 winding has time to drop to zero when the key transistor closes. In terms of reducing the ripple level, discontinuous current mode is preferable. However, the choke calculation according to the method [8] shows that the inductance for discontinuous currents mode for PWM would be in a range from 1.5 to 5.0 mH (depending on the converter frequency). Due to the considerable size, mass, and cost of such a choke, the mode of discontinuous currents with inductance of the choke of the order of 50–150 μHY in the converter. The inevitable increase in ripple was leveled by using the linear voltage regulator.

#### **SCHEMATIC CIRCUIT DIAGRAM**

The schematic circuit diagram of the DC/DC converter for powering spectral lamps is shown in Fig. 3.

Elements L1, C1, and C2 form the input filter. Choke L1 smooths the input current, thus reducing the pulse interference level of the converter power supply.

The master oscillator is made on elements DD1, R2, R4, and C3. The ripple frequency before transiting to the stabilization mode is 27.7 kHz, while the duty factor is 0.8.

The power section of the converter is built on elements R3, VT2-VT6, R6-R8, and L2. It is noteworthy the schematic feature of the power section construction that is parallel inclusion of MOSFETs VT5, VT6, and VT7 operating in the cutoff mode. The KP7173A<sup>8</sup> is one of the few Russian MOSFETs suitable for this application in terms of drain-source voltage. Unfortunately, the resistance of its open channel leaves much to be desired and can reach 2  $\Omega$  (according to data on its full analogue STP4NK60Z<sup>10</sup>). Obviously, with the drain current of 4 A and the duty factor of 0.5, the mean square value of power dissipation would be 4 W. This does not take into account losses caused by the transistor operating point being in the active mode during opening and closing of the channel. Such dissipated power is acceptable for the transistor but it forces to use coolers for it, thus reducing the converter efficiency significantly. One way to solve this problem is connecting several transistors in parallel.

Reference data on KP7173A. https://integral.by/sites/default/files/pdf/kp7173.pdf. Accessed May 20, 2023.

<sup>&</sup>lt;sup>9</sup> Manufactured by Integral, Minsk, Belarus.

STP4NK60Z datasheet: https://www.st.com/resource/en/datasheet/stp4nk60z.pdf. Accessed May 20, 2023.

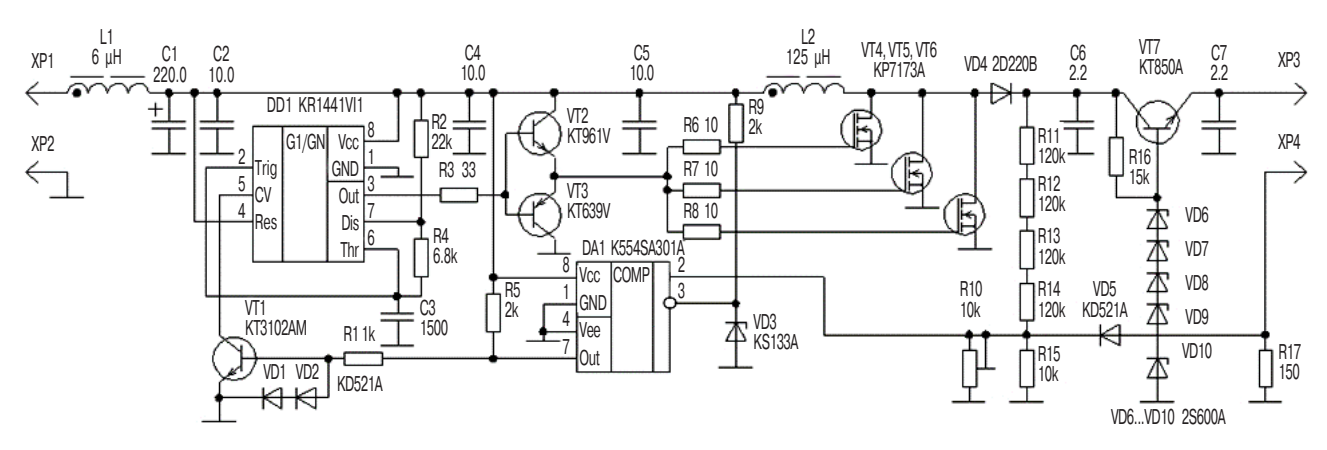


Fig. 3. Schematic circuit diagram of the DC/DC converter

Since, the transistor with the lowest resistance would be more heated because of the greater current flow even in the case of (inevitable) spread of channel resistances, parallel connection of MOSFETs is acceptable. When the temperature of the MOSFET crystal increases, the resistance of its open channel increases, thereby causing a decrease in current.

The calculation of the required number of key transistors is dictated by the current flowing through them as well as their heating.

The maximum transition temperature of the KP7173A transistor is +150°C; the "crystal-to-package" thermal resistance is 1.78 K/W. The "crystal-to-medium" thermal resistance for the KT-28-2 (TO-220) package wherein the KP7173A transistor crystal is mounted, according to various data, ranges from 50°C/W to 70°C/W. When using the converter under UHL 4.2 conditions<sup>11</sup> (maximum air temperature is +40°C), taking a margin of +25°C for heating inside the item, and selecting the maximum transition temperature of the transistor of +100°C, the permissible overheating of the package is +35°C. In the case of the "crystal-to-medium" thermal resistance of 70°C/W, a maximum power dissipation of 0.5 W is obtained. Hence, three transistors (power dissipation on each is 0.45 W, crystal temperature is 96.5°C, and package temperature is 54.2°C) would be sufficient in terms of thermal conditions without using coolers<sup>12</sup>.

Transistors VT2 (KT639V<sup>13</sup>) and VT3 (KT961V<sup>14</sup>) are driver transistors for field-effect transistors VT4, VT5, and VT6, since the MOSFET gate is a capacitance which has to be rapidly charged and discharged for

opening and closing the transistor. The total charge Q of the gate [13] for the STP4NK60Z transistor is 26 nC, as stated in its technical documentation. Knowing the total charge and the necessary time T to communicate this charge, the current intensity I is determined by the following formula:

$$I = \frac{Q}{T}. (3)$$

For the charge of 78 nC (three transistors connected in parallel) and the charge time of 100 ns, the charge current is 780 mA<sup>15</sup>. Since the output of the KR1441VI1 chip is not designed for such current, a buffer stage is required. At the same time, the current consumed by the buffer stage at the input would be  $h_{21E}$  times less than the output current. According to [14], the minimum current transfer coefficient  $h_{21E}$  for the KT961V and KT639V transistors is 100, which means that the maximum output chip current would be reduced to 7.8 mA. Resistor R5 serves to limit current while resistors R9-R11, in addition to current limiting, also suppress resonant oscillations in the "capacitance-'gate-source'-drain inductance" circuit [15]. Choke D13-14 with windings connected in series (125  $\mu$ HY, 4 A, 0.05  $\Omega$ , and 2 MHz) is used as storage choke L2. The output voltage rectification is carried out by the 2D220B-type diode VD4<sup>16</sup>.

The output voltage stabilization circuit is made on the comparator DA1, transistor VT1 and its harness, parametric voltage regulator (RVS) on stabilitron VD3 (3.3 V), and divider R11–R15. The divider R11–R15 upper arm consists of four resistors connected in series for increasing the maximum allowable applied voltage. Resistor R10 serves as a trimmer, rotating its slider to set the output voltage to 530 V. In case of its interruption the output voltage

<sup>&</sup>lt;sup>11</sup> GOST 15050-69. Machines, instruments and other industrial products. Modifications for different climatic regions. Categories, operating, storage and transportation conditions as to environment climatic aspects influence. Moscow: Standardinform; 2010 (in Russ.).

 $<sup>^{12}</sup>$  At the thermal resistance of 50°C/W, the crystal temperature is 87.5°C while the body temperature is 49.2°C.

<sup>&</sup>lt;sup>13</sup> Manufactured by GRUPPA KREMNI EL, Bryansk, Russia.

<sup>&</sup>lt;sup>14</sup> Manufactured by Integral, Minsk, Belarus.

 $<sup>^{15}\,</sup>$  The limiting case is 26 nC of gate charge; the typical value is 18.8 nC.

Manufactured by the Scientific and Production Enterprise TOMILINO ELECTRONIC PLANT, Tomilino, Russia.

Table 2. Power dissipation of parallel connected transistors

Number of transistors, items	Equivalent resistance, $\Omega$	Total power dissipation at 4 A and duty factor 0.5, W	Power dissipation per transistor in case of equal channel resistances, W	
3	0.667	1.35	0.45	
4	0.5	1.00	0.25	
5	0.4	0.80	0.20	

Table 3. Components used and their analogs

Type by scheme	Model	Analog (full or partial)	Comments
KR1441VI1	TLC555	Full	-
K554SA301A	LM311	Full	_
KP7173A	SPP20N60C3	Partial	The 1.4-ohm resistor is added to the drain for approaching $R_{\rm DS~on}$ of KP7173A, where $R_{\rm DS~on}$ is the drain-source resistance in the open state of the transistor
2D220B	DI_US1J <sup>1</sup>	Partial	Matches in capacitance, reverse voltage $U_{\text{rev}}$ , and direct current $I_{\text{dir}}$ , but has a shorter reverse recovery time (75 ns vs. 600 ns)
2S600A	PH_BZX585-B75 <sup>2</sup> , PH_BZX585-B51 <sup>20</sup>	Full	The model uses an assembly of 75 V and 51 V stabilitrons for total stabilization voltage of 601 V
KS133A <sup>3</sup>	BZX84C3V3 <sup>19</sup>	Full	-
KT961V	BD139 <sup>4</sup>	Full	-
KT639V	BD140 <sup>22</sup>	Partial	Matches in the collector-emitter voltage $U_{\rm CE}$ , collector current $I_{\rm C}$ , and cutoff frequency $F_{\rm CF}$
KT850A	BD139	Partial	Matches in $U_{\rm CE}$ , $I_{\rm C}$ , and $F_{\rm CF}$
KT3102A <sup>5</sup>	2N3904p <sup>6</sup>	Partial	Has lowest $h_{21E}$ but it does not matter in this particular case

<sup>&</sup>lt;sup>1</sup> Manufactured by Vishay, USA.

would be set to 160 V. When the converter is switched on, the output voltage starts increasing; therefore, the divider output voltage starts increasing as well. Once it equals or exceeds the reference voltage of 3.3 V, the comparator would set a high level at the output by opening transistor VT1 and closing pin 5 of chip DD1 to the common wire to prevent ripple generation. The output voltage would be maintained by the capacitive filter. As soon as the voltage at the divider output drops below 3.3 V, the comparator would set low level, closing transistor VT1, and thus enabling ripple generation again.

The output voltage capacitive filter is made on capacitor C6. The parallel connection of ten 0.22  $\mu F \times 630$  V ceramic capacitors of size 2220 with total capacitance of 2.2  $\mu F$  is used.

The linear stabilizer is made on transistor VT7 KT850A<sup>17</sup>, stabilitrons VD6-VD10 2S600A<sup>18</sup>, and the current set resistor R16. The series connection

of five diodes is used for obtaining stabilization voltage of 500 V, since the Russian industry does not produce 500 V stabilitrons.

The current protection is made on elements R18 and VD7. When the current through the load (hence, through resistor R17) exceeds 25 mA, the voltage drop across resistor R17 minus the voltage drop across diode VD5 would be 3.3 V. This will cause the comparator DD2 to set the output to the high level, thus stopping ripple generation. Diode VD5 is designed to prevent current flowing from the negative feedback divider to resistor R17.

#### **CONVERTER SIMULATION**

The simulation has been performed within the *LTSpice XVII* software [16]. The active component models given in Table 3 have been used.

The model schematic is shown in Fig. 4.

<sup>&</sup>lt;sup>2</sup> Manufactured by Nexperia, Netherlands.

<sup>&</sup>lt;sup>3</sup> Manufactured by Novosibirsk Semiconductor Device Plant, Novosibirsk, Russia.

<sup>&</sup>lt;sup>4</sup> Manufactured by ST Microelectronics, Switzerland.

<sup>&</sup>lt;sup>5</sup> Manufactured by GRUPPA KREMNI EL, Bryansk, Russia.

<sup>&</sup>lt;sup>6</sup> Manufactured by Diotec Semiconductor, Germany.

<sup>17</sup> Manufactured by GRUPPA KREMNI EL, Bryansk, Russia.

<sup>&</sup>lt;sup>18</sup> Manufactured by Novosibirsk Semiconductor Device Plant, Novosibirsk, Russia.

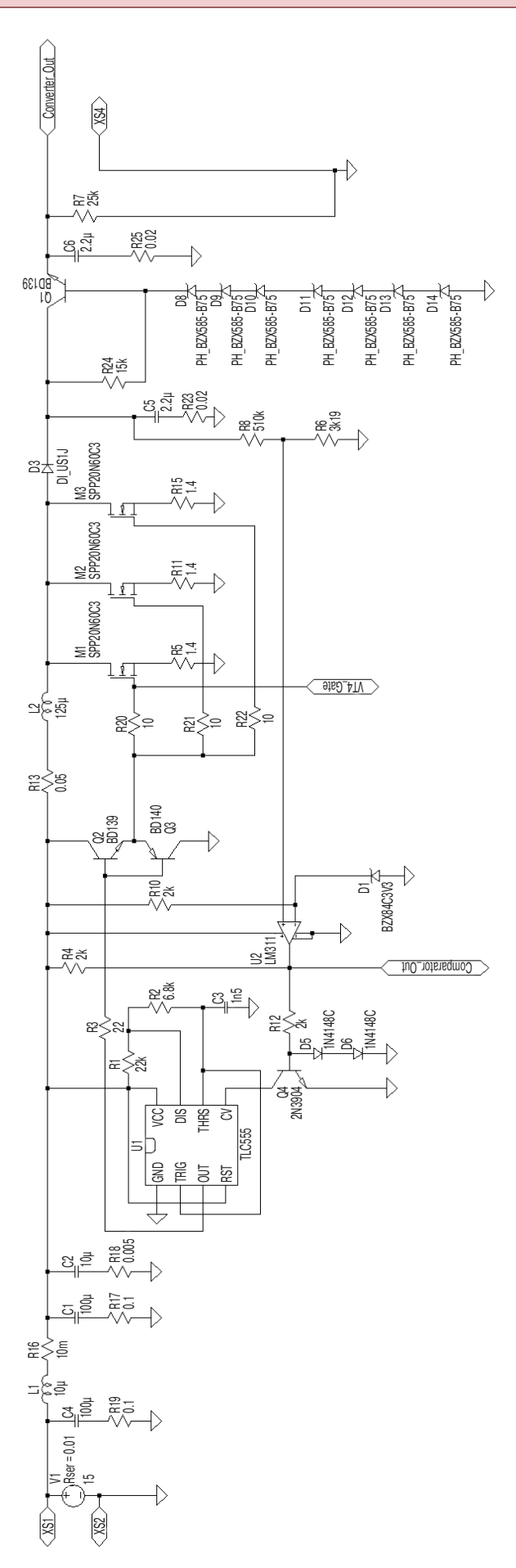
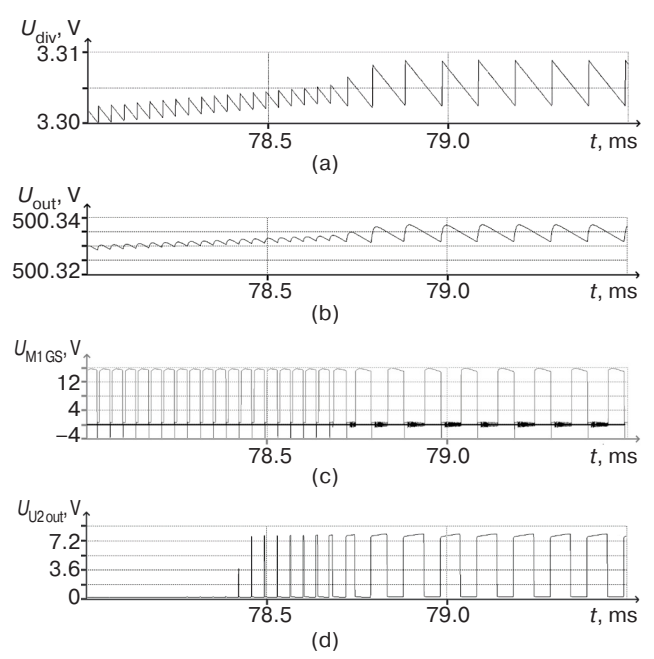


Fig. 4. Schematic diagram of the converter in LTSpice

Simulation has been performed using the .tran 0 500m 1u uic directive: transient analysis; start time of the data acquisition is 0 s; end time of the data acquisition is 0.5 s; simulation step is 1  $\mu$ s; and transients in reactivities are included.

Main characteristic diagrams are shown in Fig. 5.



**Fig. 5.** Characteristic diagrams of the converter operation: (a) feedback divider output voltage  $U_{\rm div}$ , (b) converter output voltage  $U_{\rm out}$ , (c) gate voltage of field-effect transistor M1  $U_{\rm M1\,GS}$ , (d) comparator output voltage U2  $U_{\rm U2\,out}$ 

The simulative converter reaches operating mode about 79 ms after start. At this time, the voltage at the feedback divider output  $U_{\rm div}$  reaches the level of the comparator reference voltage. The comparator output  $U_{\rm U2~out}$  is set to the "high state" level. The high signal level at the comparator output, which is formed when



Fig. 6. Assembled converter board

the output voltage reaches 500 V, causes generation to stop at the TLC555 chip output.

# ASSEMBLY AND EXPERIMENTAL VERIFICATION OF THE CONVERTER

The converter is assembled on a double-sided printed circuit board (PCB) made of foil fiberglass. The pattern of the printed tracks is made completely on the bottom side of the board. The upper side of the board is used for the common wire; thus, its resistance and inductance are minimized, which is important in pulsed high-frequency circuits [17]. The mounting is mixed. The PCB image is shown in Fig. 6.

The test bench of the converter consists of a Element PSN-305D laboratory power supply unit<sup>19</sup> providing power for the converter; a Fluke 17B+ handheld multimeter<sup>20</sup> in the voltmeter mode for measuring the output voltage; and a Uni-T UT802 bench multimeter<sup>21</sup> in the milliammeter mode for measuring the output current. A Rigol MSO 4024 digital oscilloscope<sup>22</sup> is used for taking voltage waveforms. The test bench images are shown in Figs. 7 and 8. The oscillogram of pulsations at the converter output under load is shown in Fig. 9.

- <sup>19</sup> Manufactured by Element, China.
- <sup>20</sup> Manufactured by Fluke, China.
- <sup>21</sup> Manufactured by Uni-Trend Group, China.
- <sup>22</sup> Manufactured by Rigol Technologies, China.

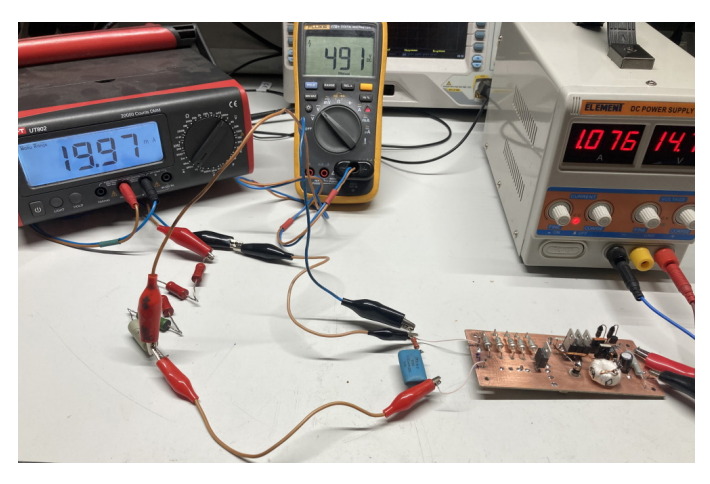


Fig. 7. Checking the load capacity of the converter

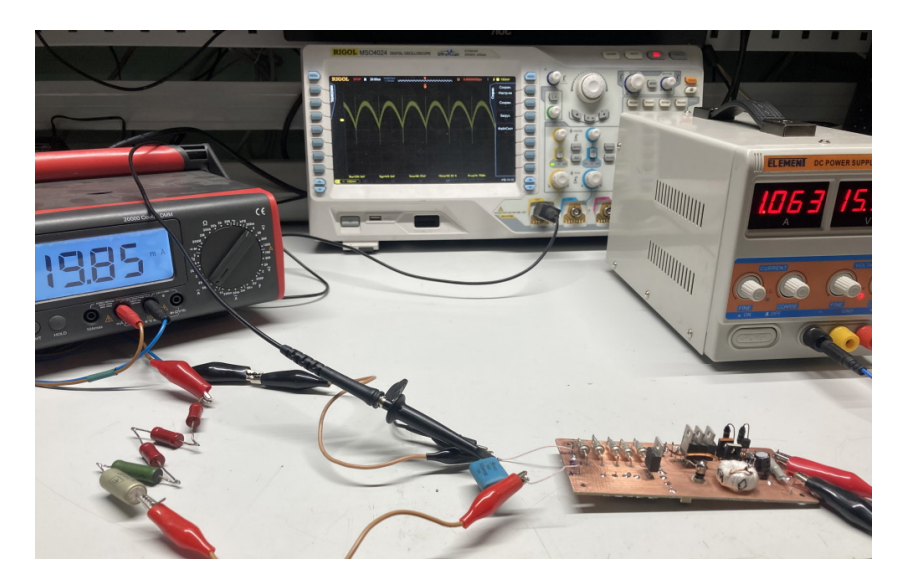


Fig. 8. Checking the ripple level at the converter output under load

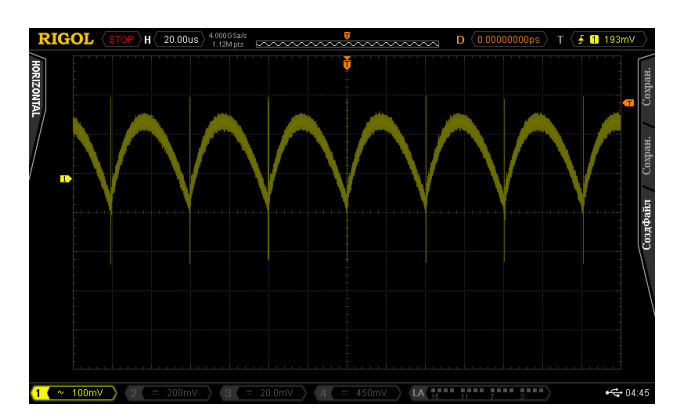


Fig. 9. Oscillogram of the output voltage ripple under load

The load capacity of the converter is confirmed by the output voltage of 491 V at a current of 20 mA. The compound resistor with total resistance of 25 k $\Omega$  is used as the load.

For checking the ripple level, the oscilloscope is connected to the converter output through the differential RC-chain with ratings of 0.022  $\mu F$  and 100  $k\Omega.$  The cutoff frequency of the high-pass filter formed by such circuit is 72 Hz at the 3 dB level.

The peak ripple level is  $250\,\mathrm{mV}$  (0.05% over  $500\,\mathrm{V}$ ), which confirms the above conclusions about the low ripple level of the converter under consideration.

#### **CONCLUSIONS**

In the paper, the results of the development, modeling, circuit assembly, and experimental study of the specialized pulse DC/DC converter for powering spectral tubes are presented. Development of the circuit diagram is carried

out with the expectation for a minimum number of tuning operations during assembly (as shown, this operation may be neglected), as well as the absence of a necessity to use a heat sink, and minimized use of imported element base. Simulation of the DC/DC converter is done partly on approximated analogs, whereby additional elements are introduced into the circuit for approximating model parameters to actually used components. The PCB for the converter is traced with allowance for minimizing the inductance and resistance of the high-frequency conductors and the common wire. The converter performance (including with an equivalent load for achieving the required output current) and the compliance of measurements with simulation results confirm the correctness of calculations and simulation. The converter provides 491 V at the current of about 20 mA and peak ripple of 250 mV (0.05%).

**Authors' contribution.** All authors equally contributed to the research work.

#### **REFERENCES**

- 1. Moskalev B.I. *Razryad s polym katodom* (*Discharge with Hollow Cathode*). Moscow: Energiya; 1969. 184 p. (in Russ.).
- 2. Maksimov D.E., Rudnevskii N.K. *Spektral'nyi analiz s primeneniem razryada v polom katode (Spectral Analysis Using Hollow Cathode Discharge*). Gor'kii: GGU; 1979. 119 p. (in Russ.).
- 3. Maksimov D.E., Rudnevskii N.K., Rudnevskii A.N., Shabanova T.M. Spektral'nyi analiz s primeneniem razryada v polom katode (Spectral Analysis Using Hollow Cathode Discharge). Gor'kii: GGU; 1983. 71 p. (in Russ.).
- 4. Garmash A.V. Vvedenie v spektroskopicheskie metody analiza. Opticheskie metody analiza (Introduction to Spectroscopic Methods of Analysis. Optical Methods of Analysis). Moscow: RAN VKhK; 1995. 38 p. (in Russ.).
- Bityukov B.K., Gorbunov R.A., Simachkov D.S., Frunze A.V. A Highly Stable Source of Spectral Lines. *Opt. Spectrosc.* 2019;126(4):450–453. https://doi. org/10.1134/S0030400X19040040
   [Original Russian Text: Bityukov B.K., Gorbunov R.A., Simachkov D.S., Frunze A.V. A Highly Stable Source of Spectral Lines. *Optika i spektroskopiya*. 2019;126(4):528–532 (in Russ.). http://doi.org/10.21883/OS.2019.04.47525.50-18]
- 6. Kaganov V.I., Bityukov V.K. Osnovy radioelektroniki i svyazi (Fundamentals of Radioelectronics and Communications). Moscow: Goryachaya liniya Telekom; 2012. 542 p. (in Russ.).
- 7. Skvortsov E.A., Simachkov D.S. High-stability radiation device based on hollow cathode lamps. In: Actual Problems and Perspectives for the Development of Radio Engineering and Infocommunication Systems (Radioinfocom 2021): Proceedings of the 5th International Scientific and Practical Conference. Moscow: RTU MIREA; 2021. P. 405–408 (in Russ.). Available from URL: https://www.elibrary.ru/aelqox
- 8. Bityukov V.K., Simachkov D.S., Babenko V.P. *Istochniki vtorichnogo elektropitaniya* (*Secondary Power Sources*). Moscow: Infra-Inzheneriya; 2020. 376 p. (in Russ.).
- 9. Babenko V.P., Bityukov V.K., Simachkov D.S. DC/DC Buck-Boost Converter with Single Inductance. *Russ. Microelectron.* 2021;50(6):471–480. https://doi.org/10.1134/S1063739721060044
- Sergeev B.S. Skhemotekhnika funktsional'nykh uzlov istochnikov vtorichnogo elektropitaniya (Schematics of Functional Units of Secondary Power Sources. Reference-book). Moscow: Radio i svyaz'; 1992. 224 p. (in Russ.).
- 11. Meleshin V.I. *Tranzistornaya preobrazovatel'naya tekhnika (Transistor Converter Technology)*. Moscow: Tekhnosfera; 2005. 632 p. (in Russ.).
- 12. Naivel't G.S., Mazel' K.B., Khusainov Ch.I., et al. *Istochniki elektropitaniya radioelektronnoi apparatury* (*Power Supply Sources REA: reference-book*). Naivelt G.S. (Ed.). Moscow: Radio i svyaz'; 1985. 576 p. (in Russ.).

#### СПИСОК ЛИТЕРАТУРЫ

- 1. Москалев Б.И. *Разряд с полым катодом*. М.: Энергия; 1969. 184 с.
- 2. Максимов Д.Е., Рудневский Н.К. *Спектральный анализ с применением разряда в полом катоде*. Горький: ГГУ; 1979. 119 с.
- 3. Максимов Д.Е., Рудневский Н.К., Рудневский А.Н., Шабанова Т.М. Спектральный анализ с применением разряда в полом катоде. Горький: ГГУ; 1983. 71 с.
- 4. Гармаш А.В. Введение в спектроскопические методы анализа. Оптические методы анализа. М.: РАН ВХК; 1995. 38 с.
- 5. Битюков В.К., Горбунов Р.А., Симачков Д.С., Фрунзе А.В. Высокостабильный источник спектральных линий. *Оптика и спектроскопия*. 2019;126(4): 528–532. http://doi.org/10.21883/OS.2019.04.47525.50-18
- 6. Каганов В.И., Битюков В.К. *Основы радиоэлектрони-ки и связи*. М.: Горячая линия-Телеком; 2012. 542 с.
- 7. Скворцов Е.А., Симачков Д.С. Устройство по созданию высокостабильного излучения на основе ламп с полым катодом. В сб.: Актуальные проблемы и перспективы развития радиотехнических и инфокоммуникационных систем «Радиоинфоком 2021»: Сборник научных статей V международной научно-практической конференции. М.: РТУ МИРЭА; 2021. С. 405—408. URL: https://www.elibrary.ru/aelgox
- 8. Битюков В.К., Симачков Д.С., Бабенко В.П. *Источни-ки вторичного электропитания*. М.: Инфра-Инженерия; 2020. 376 с.
- 9. Бабенко В.П., Битюков В.К., Симачков Д.С. Понижающе-повышающий DC/DC преобразователь с единственной индуктивностью. *Микроэлектроника*. 2022;51(1):60–70. https://doi.org/10.31857/S0544126921060041
- 10. Сергеев Б.С. Схемотехника функциональных узлов источников вторичного электропитания: Справочник. М.: Радио и связь; 1992. 224 с.
- 11. Мелешин В.И. *Транзисторная преобразовательная техника*. М.: Техносфера; 2005. 632 с.
- 12. Найвельт Г.С., Мазель К.Б., Хусаинов Ч.И. и др. *Источники электропитания радиоэлектронной ап- паратуры: Справочник*; под ред. Г.С. Найвельта. М.: Радио и связь; 1985. 576 с.
- 13. Бабенко В.П., Битюков В.К. Измерение заряда затвора для ключей на мощных MOSFET транзисторах. В сб.: Современные проблемы профессионального образования: опыт и пути решения. Материалы Второй всероссийской научно-практической конференции с международным участием. Иркутск: Иркутский государственный университет путей сообщения; 2017. С. 37–41. URL: https://www.elibrary.ru/zebetl
- 14. Зайцев А.А., Миркин А.И., Мокряков В.В. *Полупрово- дниковые приборы. Транзисторы средней и большой мощности: Справочник;* под ред. А.В. Голомедова. М.: КУбК-а; 1995. 640 с.
- 15. Новиков П. Затворный резистор. Часть 1. *Силовая* электроника. 2018;6(75):4–8.
- 16. Володин В.Я. *LTspice: компьютерное моделирование* электронных схем. СПб.: БХВ-Петербург; 2010. 400 с.

- Babenko V.P., Bityukov V.K. Gate charge measurement for high power MOSFET switches. In: Modern Problems of Vocational Education: Experience and Solutions. Materials of the Second All-Russian scientific-practical conference with international participation. 2017. Irkutsk: Irkutsk State Transport University; 2017. P. 37–41 (in Russ.).
- Zaitsev A.A., Mirkin A.I., Mokryakov V.V. Poluprovodnikovye pribory. Tranzistory srednei i bol'shoi moshchnosti (Semiconductor Devices. Medium and High Power Transistors: Handbook). Golomedov A.V. (Ed.). Moscow: KUbK-a; 1995. 640 p. (in Russ.).
- 15. Novikov P. Gate resistor. Part 1. Silovaya elektronika = Power Electronics. 2018;6(75):4–8 (in Russ.).
- 16. Volodin V.Ya. LTspice: komp'yuternoe modelirovanie elektronnykh skhem (LTspice: Computer Simulation of Electronic Circuits). St. Petersburg: BKhV-Peterburg; 2010. 400 p. (in Russ.).
- Barnes J.R. Electronic System Design: Interference and Noise Control Techniques. Transl. from Engl. Moscow: Mir; 1990. 238 p. (in Russ.).
   [Barnes J.R. Electronic System Design: Interference and Noise Control Techniques. New Jersey: Prentice Hall; 1987. 244 p.]

17. Барнс Дж. Электронное конструирование: Методы борьбы с помехами: пер. с англ. М.: Мир; 1990. 238 с.

#### About the authors

**Mikhail Yu. Nikolshin,** Postgraduate Student, Department of Radio Wave Processes and Technology, Institute of Radio Electronics and Informatics, MIREA – Russian Technological University (78, Vernadskogo pr., Moscow, 119454 Russia). E-mail: florenica@yandex.ru. RSCI SPIN-code 6339-2251, https://orcid.org/0009-0004-5353-7781

**Alexander V. Frunze,** Dr. Sci. (Eng.), Director of TERMOKONT Autonomous Non-Profit Organization for Research, Development and Implementation of Scientific and Technical Devices (42, Ozernaya ul. Moscow, 119361 Russia). E-mail: alex.fru@mail.ru. Scopus Author ID 6507641791, RSCI SPIN-code 7558-6141, https://orcid.org/0009-0006-8602-3650

**Vladimir K. Bityukov,** Dr. Sci. (Eng.), Professor, Department of Radio Wave Processes and Technology, Institute of Radio Electronics and Informatics, MIREA – Russian Technological University (78, Vernadskogo pr., Moscow, 119454 Russia). E-mail: bitukov@mirea.ru. Scopus Author ID 6603797260, ResearcherID Y-8325-2018, RSCI SPIN-code 3834-5360, https://orcid.org/0000-0001-6448-8509

#### Об авторах

**Никольшин Михаил Юрьевич,** аспирант, кафедра радиоволновых процессов и технологий Института радиоэлектроники и информатики ФГБОУ ВО «МИРЭА – Российский технологический университет» (119454, Россия, Москва, пр-т Вернадского, д. 78). E-mail: florenica@yandex.ru. SPIN-код РИНЦ 6339-2251, https://orcid.org/0009-0004-5353-7781

**Фрунзе Александр Вилленович,** д.т.н., директор, Автономная некоммерческая организация по исследованию, разработке и внедрению научно-технических приборов «Термоконт» (119361, Россия, Москва, ул. Озерная, д. 42). E-mail: alex.fru@mail.ru. Scopus Author ID 6507641791, SPIN-код РИНЦ 7558-6141, https://orcid.org/0009-0006-8602-3650

**Битюков Владимир Ксенофонтович,** д.т.н., профессор, профессор кафедры радиоволновых процессов и технологий Института радиоэлектроники и информатики ФГБОУ ВО «МИРЭА – Российский технологический университет» (119454, Россия, Москва, пр-т Вернадского, д. 78). E-mail: bitukov@mirea.ru. Scopus Author ID 6603797260, ResearcherID Y-8325-2018, SPIN-код РИНЦ 3834-5360, https://orcid.org/0000-0001-6448-8509

Translated from Russian into English by Kirill V. Nazarov Edited for English language and spelling by Thomas A. Beavitt